THEORETICAL BIOLOGY FORUM
ISSN: 2283-7175 | https://tbfpeerjournal.org/

Dynamic Analysis and Design of Motorcycle Engine Mounting System Subjected to Vibrational Loads

Saad Alqattan*, Ajay P. Rao

Department of Mechanical Engineering
Australian College of Kuwait
Block 5 - Al Aqsa Mosque Street, Kuwait

ABSTRACT

This article presents a study of a mounting system that is used to isolate vibrations in motorcycles. The isolating system consists of the powertrain assembly, swing-arm assembly and the mounts that are used for isolation. In addition to mounting the powertrain in place, engine mounts are used to minimize the transmitted forces from the engine to the frame. The governing equations of motion are being derived for a V-Twin engine which is generally used in motorcycle applications. The loads that need to be minimized are the loads due to the shaking force. These forces are generated in part as a result of the rotating unbalance due to eccentric masses and due to the acceleration of the moving masses that the reciprocating engine consists of. An optimization problem is first set up to determine the mount stiffness rates in all three principal directions. Then the effect of the varying engine speed on mount characteristics is studied. Shape optimization is also performed to find the geometrical mount shape due to the stiffness values in the principal direction of the mount.

KEYWORDS: Motorcycle mounts design; Engine mounts; Vibration isolation; Shape optimization.

INTRODUCTION

This paper discusses the V-Twin engine configuration that is commonly used in motorcycle applications. There are two sources of vibration that affect the performance of a motorcycle engine mount system; the first one is due to the shaking forces which are generated due to the engine imbalance in the moving parts inside the engine. This force is transmitted to the frame through the mounting system. The second force is due to the road loads which are caused by the irregularities in the road profile. These forces are transmitted to the frame thorough the tire patch. The road load could be periodic or non-periodic whereas the shaking load is periodic. This paper focuses on only on the shaking loads.

This work focuses on designing the most suitable mounting system that provides isolation against forces transmitted from the powertrain to the frame. It is known that force and motion isolation are the major problems that engineers encounter when designing an engine mount. Motorcycle engines contain reciprocating parts that produce shaking forces due to the movement of various parts of the engine. The main objective herein is to minimize these shaking forces. This objective is achieved by supporting the powertrain by using a resilient support or an isolator. The largest lumped mass that the vehicle carries is the powertrain, which is attached to the frame using rubber mounts. These engine mounts are generally reinforced bonded-rubber bushings (figures 1 and 2).

Figure 1. Front engine mount

A substantial amount of research has been done in the area engine mount design for automotive and aircraft applications. However, the mounting system in motorcycle applications has its own unique challenge. The

motorcycle rear suspension system is coupled to the powertrain through the shaft which to the complexity of the problem. On top of this, the motorcycle mounting system has to withstand the road loads as well. The mounting system that is used in these cases must ensure low vibration transmission from/into the engine. There are a lot of factors to consider when looking at the source of vibration, which could be internal or external or both.

Figure 2. Rear engine mount

Spiekermann, *et al.* (1985), discussed the issue of minimizing the forces that are transmitted through the mounting system. He explored the forces that are generated from the rotational imbalance and reciprocating masses. Ford (1985), presented a design procedure for the front wheel drive engine idle isolation in which a six degree of freedom lumped system is used to represent the engine mount. Swanson *at al.* (1993), studied the mounting system of aircraft engines by minimizing the loads transmitted to the frame with an addition of constraint due to the deflection present from the static weight of the engine. Ashrafiuon (1993), explored the same behavior taking into consideration the flexibility of the frame. Sui (2003) emphasized on the role of mounts in achieving better vehicle handling characteristics and rider comfort as well as a resulting vibration caused by engine firing force and other sources. Liu (2003) presents a method used in the optimization design of engine mounts. The constraint problem is solved using some of the known parameters such as engine center of gravity, mount stiffness rates and mount location and/or orientation. Courteille and Mortier (2005) present a new technique to find an optimized and robust solution for the mounting system. Multi objective algorithm (Pareto optimization) is used as a base to the multi objective robust optimization problem. The use of this technique enhances the vehicle isolation characteristics.

This paper presents a new method to design the mounting system in a motorcycle. It focuses on the internal shaking forces which are created due to the engine imbalance as the source of vibration which will be minimized. The shaking force is defined as the sum of the inertia and static forces that are transmitted to the frame through the mounting system as suggested by Kaul, (2006). The mounting system consists of a pair of mount that support the front of the powertrain and another pair supports the rear end. The optimization problem is formulated such that the mount stiffness, location and orientation are optimized. Before developing the expressions for shaking forces in a V-Twin engine, an analysis will be performed to develop expressions for shaking forces in a single cylinder engine.

The paper is organized as follows. Section 2 discusses the dynamic analysis in which the engine mount is characterized and the six DOF model is set up. Section 3 discusses the shaking forces and develops expression for the shaking forces for a single cylinder engine first, then expanding these expressions to accommodate the V-Twin engine configuration. The optimization problem formulation is presented in section 4. The concept of shape optimization is presented in section 5. Section 6 and section 7 presents the numerical results and conclusions.

DYNAMIC ANALYSIS

Figure 3 shows a schematic diagram of the powertrain along with a pair of mount used. Figure 4 shows a schematic diagram of the mount that will be used in this study. The challenge that is faced in this stage is identifying the mount properties which are represented in stiffness in all three principal directions, its location and orientation. The model represented in Fig. 4 is a simple Voigt model that consists of a rigid body that resembles the powertrain which is connecting to the frame using the mounting system. The stiffness k and the damper c represent a single D.O.F system with an equation of motion shown in Eq. (1).

$$M\ddot{x} + C\dot{x} + Kx = Fe^{i\omega t} \quad (1)$$

In the Eq. (1), F denotes the input force vector that can be caused be either the shaking force or the road load or both. M, C and K represent the mass, damping and stiffness matrices respectively whereas x represents the displacement vector.

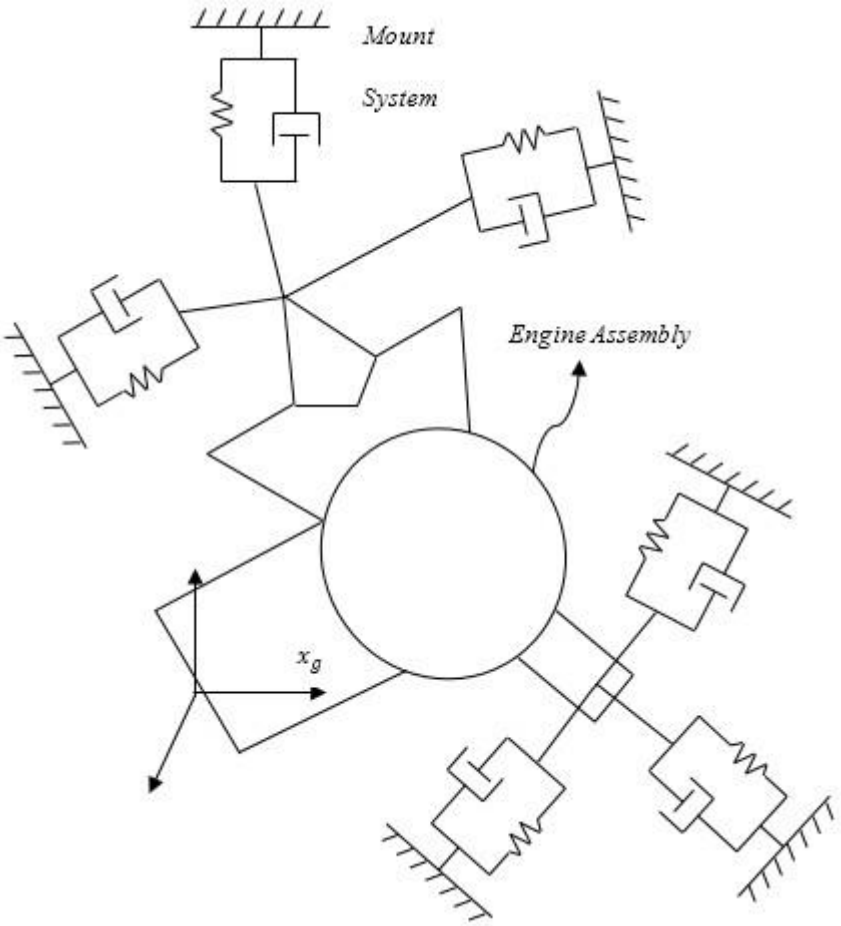

Figure 3. Schematic diagram of the engine

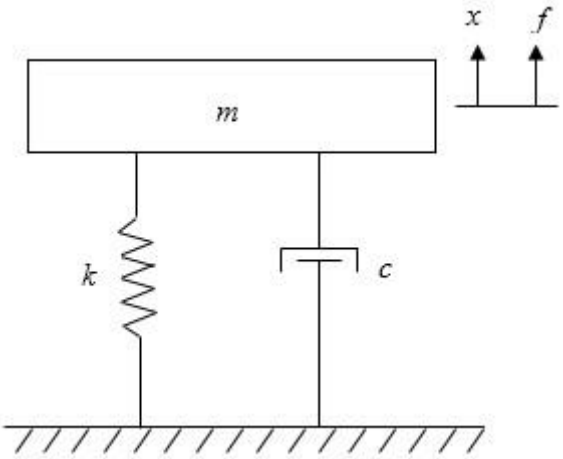

Figure 4: Schematic diagram of the mount model.

The terms of the inertia matrix *M* of the powertrain are with respect of the global coordinate system. In order to account for different orientations of the mounts; the stiffness and damping which are represented in the local coordinate system of the mount must be expressed in the global coordinate system which is achieved by using a transformation matrix. The mass matrix of the powertrain is represented in Eq. (2).

$$M_{p.t} = \begin{bmatrix} m_e & 0 & 0 & 0 & m_e z_e & -m_e y_e \\ 0 & m_e & 0 & -m_e z_e & 0 & m_e x_e \\ 0 & 0 & m_e & m_e y_e & -m_e x_e & 0 \\ 0 & -m_e z_e & m_e y_e & I_{xxe} & -I_{xye} & -I_{xze} \\ m_e z_e & 0 & -m_e x_e & -I_{xye} & I_{yye} & -I_{yze} \\ -m_e y_e & m_e x_e & 0 & -I_{xze} & -I_{yze} & I_{zze} \end{bmatrix} \quad (2)$$

In Eq. (2), $M_{p.t}$ is the mass of the powertrain assembly, (x_e, y_e, z_e) is the location of the center of gravity of the powertrain with respect to the origin of the coordinate system and I_{xxe}, I_{yye}, I_{zze}, … are the inertia of the powertrain with respect to the origin of the coordinate system. The stiffness and damping matrices of an individual mount expressed about its own coordinate system is given by Eqs. (3) and (4).

$$k_i^* = \begin{bmatrix} k_{xi} & 0 & 0 \\ 0 & k_{yi} & 0 \\ 0 & 0 & k_{zi} \end{bmatrix} \quad (3)$$

$$c_i^* = \begin{bmatrix} c_{xi} & 0 & 0 \\ 0 & c_{yi} & 0 \\ 0 & 0 & c_{zi} \end{bmatrix} \quad (4)$$

A transformation matrix (A) is used in order to transfer both, the stiffness and damping matrices to the global coordinate system as follows:
$k_i = A_i^T k_i^* A_i$ and $c_i = A_i^T c_i^T A_i$ where c_i and k_i are the individual mount damping and stiffness matrices expressed in the global coordinate system. The matrix A_i is a transformation matrix which is a combination of the three different rotations θ_1, θ_2 and θ_3 about x, y and z axes with respect to the global coordinate system.

$$A_i = \begin{bmatrix} C\theta_{2i}C\theta_{3i} & -C\theta_{1i}S\theta_{3i} + S\theta_{1i}S\theta_{2i}C\theta_{3i} & S\theta_{1i}S\theta_{3i} + C\theta_{1i}S\theta_{2i}C\theta_{3i} \\ C\theta_{2i}S\theta_{3i} & C\theta_{1i}C\theta_{3i} + S\theta_{1i}S\theta_{2i}S\theta_{3i} & S\theta_{1i}S\theta_{3i} + C\theta_{1i}S\theta_{2i}C\theta_{3i} \\ -S\theta_{2i} & S\theta_{1i}C\theta_{2i} & C\theta_{1i}C\theta_{2i} \end{bmatrix} \quad (5)$$

In Eq. (5) $C\theta_i = cos(\theta_i)$ and $S\theta_i = sin(\theta_i)$.
The transformed damping and stiffness matrices are shown in Eq. (6)

$$C_e = \begin{bmatrix} C_{11} & C_{12} \\ C_{21} & C_{22} \end{bmatrix}, \; K_e = \begin{bmatrix} K_{11} & K_{12} \\ K_{21} & K_{22} \end{bmatrix} \quad (6)$$

$$K_{11} = \sum k_i, \quad K_{12} = -\sum k_i \tilde{r}_i, \; K_{21} = K_{12}$$
$$K_{22} = -\sum \tilde{r}_i k_i \tilde{r}_i \quad (7)$$

$$C_{11} = \sum c_i, \quad C_{12} = -\sum c_i \tilde{r}_i, \; C_{21} = C_{12}$$
$$C_{22} = -\sum \tilde{r}_i c_i \tilde{r}_i \quad (8)$$

K_e and C_e represents the overall damping and stiffness matrices of the powertrain assembly shown in Eq. (6). $\tilde{r}_i$ represents the skew-symmetric matrix that corresponds to an individual mount position (r_{xi}, r_{yi}, r_{zi}) and it's given by:

$$\tilde{r}_i = \begin{bmatrix} 0 & -r_{zi} & r_{yi} \\ r_{zi} & 0 & -r_{xi} \\ -r_{yi} & r_{xi} & 0 \end{bmatrix} \quad (9)$$

In this paper, a six degree of freedom (DOF) model is used to describe the powertrain as a rigid body. In the case, the powertrain and the exhaust system which are fixed to the frame via four mount system. The frame is assumed to be infinitely rigid. The overall equation of motion (EOM) of the six DOF is given as follows:

$$M_e \ddot{X}_e + C_e \dot{X}_e + K_e X_e = F_e e^{j\omega t} \quad (10)$$

In Eq. (10), M_e, C_e and K_e are *6* x *6* mass, damping and stiffness matrices respectively. F_e denotes the force vector at frequency ω due to the engine shaking force caused by engine imbalance described in which will be discussed in the next section. The generalized mass matrix is defined with respect to the center of gravity of the powertrain. X_e is a *6* x *1* vector that contains three translational displacements x, y and z and three rotational displacements α, β and γ of the powertrain. To account for different orientations for each mount, the stiffness and damping matrices

are assembled in their local coordinate systems and then transformed to the global coordinate system using the Eq. (3) to Eq. (9).

SHAKING FORCES

In this section, development of the shaking forces in a single cylinder engine is done first, and then all the expression are expanded to accommodate the V-Twin configuration.

Shaking Forces in a Single Cylinder Engine

Figure 5 shows a schematic diagram of a single cylinder slider crank mechanism. The standard slider crank mechanism is the basic building block of virtually all internal combustion engines. Presented next is the position, velocity, acceleration and the forces analysis of the slider-crank mechanism. Let the crank radius be r and the connecting rod length be l. The crank angle is θ and the angle that the connecting rod makes with the x axis is ϕ, the crank rotates at a constant speed ω then:

$$q = r\ \sin\theta = l\ \sin\phi \tag{11}$$

$$\theta = \omega t \tag{12}$$

$$\sin\phi = \frac{r}{l}\sin\omega t \tag{13}$$

$$s = r\ \cos\omega t \ \text{ and } u = l\ \cos\phi \tag{14}$$

The distance x that is measured from the pivot point O to the slider at point B is given as follows:

$$x = s + u = r\ \cos\omega t + l\ \cos\phi \tag{15}$$

$$\cos\phi = \sqrt{1 - sin^2\phi} = \sqrt{1 - \left(\frac{r}{l}\sin\omega t\right)^2} \tag{16}$$

$$x = r\,cos\omega t + l\sqrt{1 - \left(\frac{r}{l}\,sin\omega t\right)^2} \tag{17}$$

The expression given by Eq. (17) gives the position of the piston along the x axis as a function of crank angle θ. If a derivative of Eq. (17) is taken once with respect to time, the velocity of the piston will be determined as shown below:

$$\dot{x} = -r\omega\left[\sin\omega t + \frac{r}{2l}\frac{\sin 2\omega t}{\sqrt{1 - \left(\frac{r}{l}\sin\omega t\right)^2}}\right] \tag{18}$$

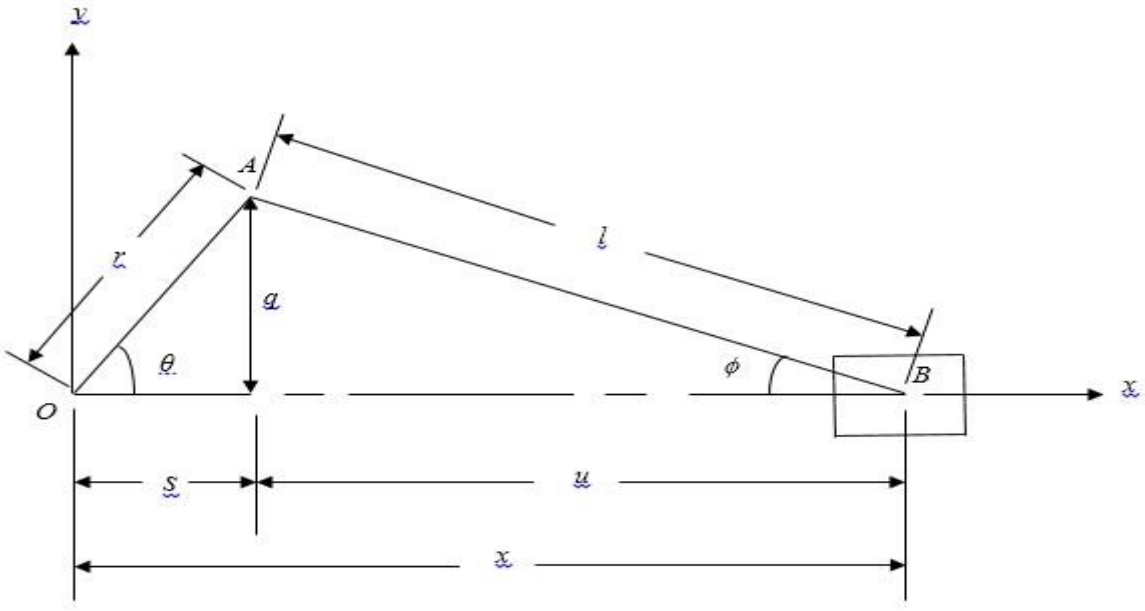

Figure 5. Slider Crank Mechanism

If a derivative of the piston velocity is taken once with respect to time, the piston acceleration is obtained as shown below:

$$\ddot{x} = -r\omega^2 \left\{ \cos\omega t - \frac{r[l^2\,(1 - 2cos^2\omega t) - r^2\,sin^4\omega t]}{[l^2 - (r\,sin\omega t)^2]^{\frac{3}{2}}} \right\} \tag{19}$$

In the velocity expression shown in Eq. (18) and the acceleration expression shown in Eq. (19), a steady state solution is considered where it is assumed that the crank speed ω is constant.

Using the binomial theorem, an approximate expression for the position, velocity and acceleration of the piston can be written as follows:

$$\begin{aligned} x &\cong l - \frac{r^2}{4l} + r\left(\cos\omega t + \frac{r}{4l}\cos 2\omega t\right) \\ \dot{x} &\cong -r\omega\left(\sin\omega t + \frac{r}{2l}\sin 2\omega t\right) \\ \ddot{x} &\cong -r\omega^2\left(\cos\omega t + \frac{r}{l}\cos 2\omega t\right) \end{aligned} \tag{20}$$

The inertia force F_i is the sum of the inertia forces at points *A* and *B* on the slider crank mechanism.

$$F_i = m_A\,a_A + m_B\,a_B \tag{21}$$

In Eq. (21), the acceleration term a_B is the acceleration of the piston which is given in Eq. (20). The acceleration term a_A could be found by taking the second derivative of the position vector at point *A* with respect to time. The position vector that describes the location of point *A* is given as follows:

$$R_A = r\cos\omega t\ \hat{\imath} + r\sin\omega t\,\hat{\jmath} \tag{22}$$

Differentiate the position vector given in Eq. (22) twice with respect to time and an expression for the acceleration at point *A* is achieved as follows:

$$a_A = [-r\alpha\ \sin\omega t - r\omega^2\cos\omega t]\,\hat{\imath} + [r\alpha\ \cos\omega t - r\omega^2\sin\omega t]\,\hat{\jmath} \tag{23}$$

In Eq. (22), $\hat{\imath}$ and $\hat{\jmath}$ are unit vectors defined along the *x* and *y* axis. The inertia force along the *x* and *y* axis are given as follows:

$$\begin{aligned} F_{ix} &= -(m_A + m_B)\,r\omega^2\,cos\omega t - m_B\frac{r^2\omega^2}{l}\,cos2\omega t \\ &\quad -(m_A + m_B)\,r\alpha\,sin\omega t - m_B\frac{r^2\alpha}{2l}\,sin2\omega t \\ F_{iy} &= m_A\,r\alpha\,cos\omega t - m_A\,r\omega^2\,sin\omega t \end{aligned} \tag{24}$$

In Eq. (24), m_A and m_B are the equivalent rotating and reciprocating masses respectively. The shaking force is $F_s = -F_i$. It is fully described taking into account the equivalent balancing masses as shown below:

$$\begin{aligned} F_{sx} &= (m_A + m_B - m_{cb})\,r\omega^2\,cos\omega t + m_B\frac{r^2\omega^2}{l}\,cos2\omega t \\ &\quad +(m_A + m_B - m_{cb})\,r\alpha\,sin\omega t + m_B\frac{r^2\alpha}{2l}\,sin2\omega t \\ F_{sy} &= (m_A - m_{cb})\,r\omega^2\,sin\omega t - (m_A - m_{cb})\,r\alpha\,cos\omega t \end{aligned} \tag{25}$$

In Eq. (25), F_{sx} and F_{sy} denote the net shaking forces in the *x* and *y* directions respectively and m_{cb} is the equivalent mass. These shaking forces result from a single cylinder.

Shaking Forces in a V-Twin Engine

Presented next is the development of shaking force expressions for a V-twin engine shown in Fig. 6. The shaking force analysis that was done on a single cylinder engine is generalized to accommodate the V-twin engine and the shaking forces will be computed along the global *X*-*Y* coordinate system.

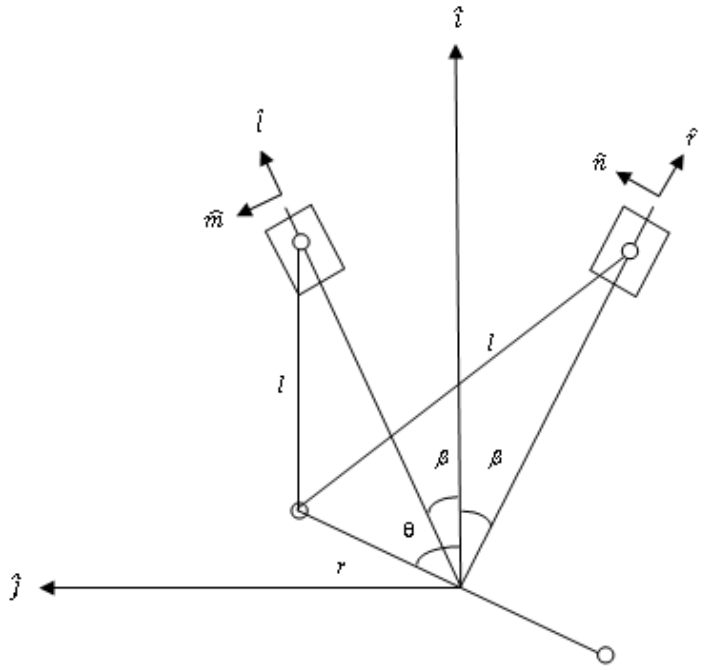

Figure 6. V-twin Engine Configuration.

In order to determine the shaking forces for the V-Twin engine, the shaking force expression for single cylinder engine given in Eq. (25) are used. The forces in each bank will be computed separately. Then by combining the corresponding terms of the shaking forces in each bank, the total shaking forces and moments can be computed in the global *X-Y* coordinate system for the V-Twin engine.

The shaking force in the left cylinder (bank) $(F_s)_{left}$ is given as follows:

$$\begin{aligned}(F_s)_{left} = \Big\{&(m_A + m_B)r\omega^2\cos(\theta-\beta) - m_{cb1}r_1\omega^2\cos(\theta-\beta) + m_B\frac{r^2\omega^2}{l}\cos2(\theta-\beta)\\ &+ (m_A + m_B)r\alpha\sin(\theta-\beta) - m_{cb1}r_1\alpha\sin(\theta-\beta) + m_B\frac{r^2\alpha}{2l}\sin2(\theta-\beta)\Big\}\hat{l}\\ &+ \{m_A r\omega^2\sin(\theta-\beta) - m_{cb1}r_1\omega^2\sin(\theta-\beta) - m_A r\alpha\cos(\theta-\beta)\\ &+ m_{cb1}r_1\alpha\cos(\theta-\beta)\}\hat{m} \qquad (26)\end{aligned}$$

$$\begin{aligned}(F_s)_{right} = \Big\{&(m_A + m_B)r\omega^2\cos(\theta+\beta) - m_{cb2}r_2\omega^2\cos(\theta+\beta) + m_B\frac{r^2\omega^2}{l}\cos2(\theta+\beta)\\ &+ (m_A + m_B)r\alpha\sin(\theta+\beta) - m_{cb2}r_2\alpha\sin(\theta+\beta) + m_B\frac{r^2\alpha}{2l}\sin2(\theta+\beta)\Big\}\hat{r}\\ &+ \{m_A r\omega^2\sin(\theta+\beta) - m_{cb2}r_2\omega^2\sin(\theta+\beta) - m_A r\alpha\cos(\theta+\beta)\\ &+ m_{cb2}r_2\alpha\cos(\theta+\beta)\}\hat{n} \qquad (27)\end{aligned}$$

In Eq. (26) and Eq. (27), $\hat{r}$ *and* $\hat{n}$ are the unit vectors along the *x* and *y* axis of the local coordinate system for the right cylinder. $\hat{l}$ *and* $\hat{m}$ are the unit vectors along the *x* and *y* local coordinate system for the left cylinder. m_{cb1} and m_{cb2} are the equivalent masses at distances r_1 and r_2 for the left and right banks respectively. Combining the shaking forces for the right and left cylinders in their corresponding local coordinate system and transferring them into the global coordinate system *X-Y* to come up with the overall shaking forces of the V-twin engine yields:

$$\begin{aligned}F_{sx} = &\sin\beta\{2(m_A+m_B)r\omega^2\sin\theta\sin\beta - 2(m_A+m_B)r\alpha\cos\theta\sin\beta\\ &+ 2m_B\frac{r^2\omega^2}{l}\sin2\theta\sin2\beta - m_B\frac{r^2\alpha}{l}\cos2\theta\sin2\beta\Big\}\\ &+ \omega^2\sin\beta\{m_{cb2}r_2\cos(\theta+\beta) - m_{cb1}r_1\cos(\theta-\beta)\}\\ &+ \alpha\sin\beta\{m_{cb2}r_2\sin(\theta+\beta) - m_{cb1}r_1\sin(\theta-\beta)\}\\ &+ \cos\beta\{2m_A r\omega^2\sin\theta\cos\beta - 2m_A r\alpha\cos\theta\cos\beta\}\\ &+ \alpha\cos\beta\{m_{cb1}r_1\cos(\theta-\beta) + m_{cb2}r_2\cos(\theta+\beta)\}\\ &- \omega^2\cos\beta\{m_{cb1}r_1\sin(\theta-\beta) + m_{cb2}r_2\sin(\theta+\beta)\} \qquad (28)\\ F_{sy} = &\cos\beta\{2(m_A+m_B)r\omega^2\cos\theta\cos\beta + 2(m_A+m_B)r\alpha\sin\theta\cos\beta\end{aligned}$$

$$+ 2m_B \frac{r^2\omega^2}{l} cos2\theta cos2\beta + m_B \frac{r^2\alpha}{l} sin2\theta cos2\beta \Big\}$$
$$- \omega^2 cos\beta \{m_{cb1} r_1 cos(\theta - \beta) + m_{cb2} r_2 cos(\theta + \beta)\}$$
$$- \alpha cos\beta \{m_{cb1} r_1 sin(\theta - \beta) + m_{cb2} r_2 sin(\theta + \beta)\}$$
$$+ sin\beta \{2m_A r\omega^2 cos\theta sin\beta + 2m_A r\alpha sin\theta sin\beta\}$$
$$+ \alpha sin\beta \{m_{cb2} r_2 cos(\theta + \beta) - m_{cb1} r_1 cos(\theta - \beta)\}$$
$$+ \omega^2 sin\beta \{m_{cb1} r_1 sin(\theta - \beta) - m_{cb2} r_2 sin(\theta + \beta)\} \quad (29)$$

The shaking forces shown in Eq. (28) and Eq. (29) can be employed to find the shaking moments by multiplying each term by the moment arm. The moments exist within each bank and their vectors will be orthogonal to the cylinder planes. For the right bank, a moment unit vector $\hat{n}$ is defined which is perpendicular to the unit vector $\hat{r}$. Similarly, a moment unit vector $\hat{m}$ is defined which is perpendicular to the unit vector $\hat{l}$ for the left bank as shown in Fig. 2.

The shaking moment in the left cylinder (bank) $(M_s)_{left}$ is given as follows:

$$(M_s)_{left} = \Big\{(m_A + m_B) r\omega^2 cos(\theta - \beta) - m_{cb1} r_1 \omega^2 cos(\theta - \beta) + m_B \frac{r^2\omega^2}{l} cos2(\theta - \beta)$$
$$+ (m_A + m_B) r\alpha sin(\theta - \beta) - m_{cb1} r_1 \alpha sin(\theta - \beta)$$
$$+ m_B \frac{r^2\alpha}{2l} sin2(\theta - \beta)\Big\} z\,\hat{m} \quad (30)$$

The shaking moment in the right cylinder (bank) $(M_s)_{right}$ is given as follows:

$$(M_s)_{right} = \Big\{(m_A + m_B) r\omega^2 cos(\theta + \beta) - m_{cb2} r_2 \omega^2 cos(\theta + \beta) + m_B \frac{r^2\omega^2}{l} cos2(\theta + \beta)$$
$$+ (m_A + m_B) r\alpha sin(\theta + \beta) - m_{cb2} r_2 \alpha sin(\theta + \beta)$$
$$+ m_B \frac{r^2\alpha}{2l} sin2(\theta + \beta)\Big\} z\,\hat{n} \quad (31)$$

In Eq. (30) and Eq. (31), z is the moment arm. Combining the shaking moments for the right and left cylinders that have been shown Eq. (30) and Eq. (31) in their corresponding local coordinate system and transferring them into the global coordinate system X-Y to come up with the overall shaking moments for the V-twin engine yields:

$$M_{sx} = cos\beta \Big\{2(m_A + m_B) r\omega^2 cos\theta cos\beta + 2m_B \frac{r^2\omega^2}{l} cos2\theta cos2\beta$$
$$+ 2(m_A + m_B) r\alpha sin\theta cos\beta + m_B \frac{r^2\alpha}{l} sin2\theta cos2\beta\Big\}.z$$
$$- \omega^2 cos\beta \{m_{cb1} r_1 cos(\theta - \beta) + m_{cb2} r_2 cos(\theta + \beta)\}.z$$
$$- \alpha cos\beta \{m_{cb1} r_1 sin(\theta - \beta) + m_{cb2} r_2 sin(\theta + \beta)\}.z \quad (32)$$
$$M_{sy} = sin\beta \Big\{-2(m_A + m_B) r\omega^2 sin\theta sin\beta - 2m_B \frac{r^2\omega^2}{l} sin2\theta sin2\beta + 2(m_A + m_B) r\alpha cos\theta sin\beta$$
$$+ m_B \frac{r^2\alpha}{l} cos2\theta sin2\beta\Big\}.z$$
$$+ \omega^2 sin\beta \{m_{cb1} r_1 cos(\theta - \beta) - m_{cb2} r_2 cos(\theta + \beta)\}.z$$
$$+ \alpha sin\beta \{m_{cb1} r_1 sin(\theta - \beta) - m_{cb2} r_2 sin(\theta + \beta)\}.z \quad (33)$$

The shaking torque of one cylinder is calculated using the inertia force acting on the piston F_{i14} multiplied by the distance x from the piston at point B to the origin of the coordinate system at point O as shown in Fig. 5. The free body diagram of the piston showing all the acting forces are shown below in Fig. 7.

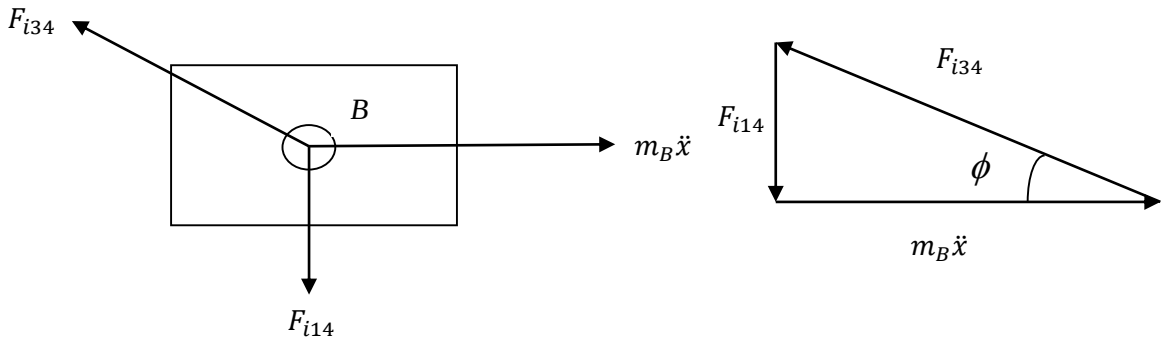

Figure 7. Free Body Diagram of the Piston

$$T_s = (F_{i14} * x)\hat{k} = m_B\ddot{x}\, tan\emptyset * x \quad (34)$$

In Eq. (34), $\ddot{x}$ is the piston acceleration represented in Eq. (5.10). Substitute the piston acceleration expressed in Eq. (5.10) into Eq. (20), the shaking torque will be expressed as follows:

$$T_s = m_B\left[-r\omega^2\left(cos\omega t + \frac{r}{l}cos2\omega t\right) - r\alpha\left(sin\omega t + \frac{r}{2l}sin2\omega t\right)\right] tan\emptyset * l - \frac{r^2}{4l} + r\left[cos\omega t + \frac{r}{4l}cos2\omega t\right] \quad (35)$$

$$tan\emptyset \approx \frac{r}{l}\, sin\omega t\left(1 + \frac{r^2}{2l^2}sin^2\omega t\right) \quad (36)$$

In Eq. (35), x is described in Eq. (20) and $\hat{k}$ is unit vector acting along the z axis which is perpendicular to the plane of the slider crank mechanism shown in Fig. 5. Assume that the angular acceleration α is zero and approximating $tan\ \phi$ as shown in Eq. (36) we get an expression for the shaking torque for both the left and the right banks.

The shaking torque in the left bank $(T_s)_{left}$ is as follows:

$$(T_s)_{left} = \frac{1}{2}m_B r^2\omega^2\left[\frac{r}{2l}sin(\theta-\beta) - sin2(\theta-\beta) - \frac{3r}{2l}sin3(\theta-\beta)\right]\hat{k} \quad (37)$$

The shaking torque in the right bank $(T_s)_{right}$ is as follows:

$$(T_s)_{right} = \frac{1}{2}m_B r^2\omega^2\left[\frac{r}{2l}sin(\theta+\beta) - sin2(\theta+\beta) - \frac{3r}{2l}sin3(\theta+\beta)\right]\hat{k} \quad (38)$$

The combined shaking torque T_s due to shaking torque from both left and right banks is the algebraic sum of both $(T_s)_{left}$ and $(T_s)_{right}$ shown below:

$$T_s = \frac{1}{2}m_B r^2\omega^2\left[\frac{r}{l}sin\theta cos\beta - 2sin2\theta cos2\beta - \frac{3r}{l}sin3\theta cos3\beta\right]\hat{k} \quad (39)$$

The final shaking force vector is a *6x1* vector shown below:

$$F_s = \begin{bmatrix} F_{sx} & F_{sy} & F_{sz} & M_{sx} & M_{sy} & T_s \end{bmatrix}^T \quad (40)$$

OPTIMIZATION PROBLEM

The optimization problem for the model represented in Fig. 4, is perused using the Sequential Quadratic Programming (SQP) technique described in Rao (2009). The objective function is formulated such that the transmitted forces are minimized taking into consideration the constraints imposed on the engine displacement due to the static and dynamic loads. The objective function that is used in this work is the weighted sum of the transmitted force through the individual mount. The transmitted forces through the mounts are due to the shaking forces generated inside the engine. The force transmitted to the frame through the individual mount is given as follows:

$$f_i = \begin{bmatrix} -k_i^* & k_i^*\,\tilde{r}_i \end{bmatrix}\begin{bmatrix} X_{ti} \\ X_{ri} \end{bmatrix} \quad (41)$$

X_{ti} and X_{ri} represents the translational and rotational displacement at the center of gravity of the powertrain as result of the shaking load. k_i^* is the local stiffness matrix for the individual mount and $\tilde{r}_i$ is the skew symmetric from the position vector of the individual mount represented in Eq. (9). The objective f_w function is assembled by summing the Euclidean norm of the individual force transmitted through each mount.

$$f_w = \sum_j \lambda_j \sum_i \|f_i\| \quad (42)$$

In Eq. (42), λ_i is the weighting parameter that corresponds to different loading conditions.

The maximum engine deflection that is allowed creates the constraints on the optimization problem. The static deflection, X_{st} is calculated at the origin of the coordinate system is calculated as:

$$X_{st} = K^{-1}F_{st} \quad (43)$$

where F_{st} is the static load acting on the system.
The engine mounts optimization problem therefore, can be stated as follows:

$$Min\ f_w(k_i, r_i, \theta_i) \quad (44)$$
$$subject\ to\ g_j(k_i, r_i, \theta_i) \leq 0 \quad j = 1, \dots, N$$

In Eq. (44), the mount stiffness, location and orientation (k_i, r_i, θ_i) are the design variables that are subjected to a total of N number of constraints g_j. The constraints that are used in the above problem consist of constraints on the engine mount stiffness, constraints on the mount location based on the available space, constraints on the mount orientation that is dictated by symmetry and finally a constraint on the deflection of the center of gravity of the powertrain due to the static weight of the powertrain. The objective function f_w is defined in Eq. (23). Both f_w and g_j are functions of the design variables (k_i, r_i, θ_i).

SHAPE OPTIMIZATION

The geometric dimensions of the isomeric mount shown in Fig. 8 are determined via a parametric study. These optimum values for the dimensions are chosen such that a complete ~~deception~~ description of the mount is achieved. The mount final shape is determined by minimizing the difference between the mount stiffness values obtained from the dynamic analysis performed in the previous section and the mount stiffness values based on its geometry which can be found from the finite element analysis. The objective function that is employed herein is described in Eq. 45 must satisfy alongside with the bound on the design variables the condition described in Eq. 46, where x_i is the i^{th} design variable and n is the number of the design variables mentioned in Kim (1997).

$$\psi = wt(1)(k_x - k_x^{des})^2 + wt(2)\left(k_y - k_y^{des}\right)^2 + wt(3)(k_z - k_z^{des})^2 \quad (45)$$
$$x_i^{min} \leq x_i \leq x_i^{max}\ for\ i = 1, \dots, n \quad (46)$$

In Eq. (45), $wt(i)$ is the weighting function that corresponds to the stiffness in the i^{th} direction. The superscript *'des'* indicates the desired stiffness that is obtained from the dynamic analysis of the mounting system, meanwhile the design parameters selected will determine the stiffness values for the geometry that is obtained from the nonlinear finite element analysis. The process of determining the design variables is expensive and time consuming, therefore in order to reduce the number of function evaluations, the least effective stiffness could be dropped from the objective function ψ.

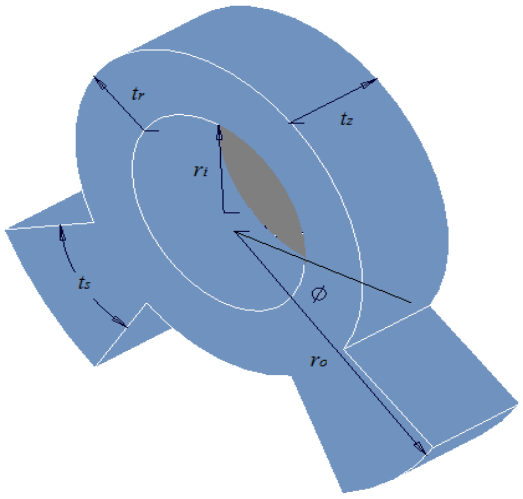

Figure 8. Schematic of a rubber mount

Figure 8, shows the actual geometry of an engine mount that is used in cars along with its defining parameters. This mount is a bush type that is made of rubber. There are a total of six parameters that dictates the shape of the mount in which four are used as the design variables namely t_s, t_z, t_r and θ. The other two parameters (r_i and r_o) are constants. These design variables affects the mount stiffness directly. The weighting function that is used in the objective function could be used to take into account the importance of the stiffness in a particular direction. The dynamic analysis is done for a motor cycle powertrain in which is supported by four isomeric mounts. The connection between the powertrain and the swing-arm are taken into consideration generating a twelve DOF system. The exciting force is limited to the internal shaking force at 4000 rpm.

In this work, the stiffness values are obtained using a nonlinear finite element analysis. The geometry shown in Fig. 8 is used to generate a mesh for the analysis. The optimization is carried out using ANSYS. Solid 186 is the element that has been used for this purpose. Appropriate boundary conditions has been applied to the model which is assumed to exhibit small deflections, for this reason the Mooney Rivlin model is sufficient to describe the fully incompressible hyperelastic material behavior of rubber as presented by Kim (1997) and Rivlin, (1992). The Mooney Rivlin model of the strain energy is expressed as:

$$U = C_{10}(I_1 - 3) + C_{01}(I_2 - 3) \quad (47)$$

I_1 and I_2 are the first and second strain invariants. The coefficients C_{10} and C_{01} are determined from the uniaxial tension test. The rubber that is used in this work is carbon black filled natural rubber. The values of the coefficients are:
C_{10} = 0.03622 and C_{01} = -0.00335.

All the design variables must satisfy the design range which could be considered as inequality constraints that dictates the lower and upper bound of these variables. Each one of these ranges that specify the upper and lower limit of the design variables are considered as inequality constraints and are incorporated in the finite element optimizer. The static deflection that is due to the static weight of the engine is measured along the axis of gravity.

$$\delta = \left|\frac{F_g}{k}\right| \quad (48)$$

F_g represents the static weight of the engine due to gravity and k represents the stiffness in the gravity direction.

NUMERICAL EXAMPLE

In this example, the force transmitted through the engine mounts due to the shaking force at 4000 rpm is used to formulate the objective function shown in Eq. (42). The mounting system used the example herein is based on four identical mounts with a circular cross section as shown in Fig. 9. The design vector contains the individual mount stiffness, orientation and position. Lower and upper bound for the design variables are listed in Table 1. Deflection constraints on the powertrain are considered due to the static and dynamic loads. The static constraints which are placed on the deflection of the powertrain are as follows:

$$|U_{st}| \leq U_{max} \quad (49)$$

In Eq. (49), U_{st} represents the static deflection of the powertrain at its *C.G.* due to the static load and U_{max} represents the maximum allowable deflection due to the static load. For this example $U_{max} = [0.025^{"}\ 0.05^{"}\ 0.025^{"} 0.5^{o}\ 0.5^{o}\ 0.5^{o}]$. An additional constraint is placed on the maximum displacement at the mount location in the y direction of *0.05 in* to prevent premature snubbing. The shaking force at 4000 rpm and the static load vector due to the engine weight are given by Eq. (50) and Eq. (51) respectively.

$$F_s = [3278\ \ 7720\ \ 0\ \ 0\ \ 0\ \ 303.8]^T \quad (50)$$

$$F_{st} = [0\ -250\ 0\ 0\ 0\ 0]^T \quad (51)$$

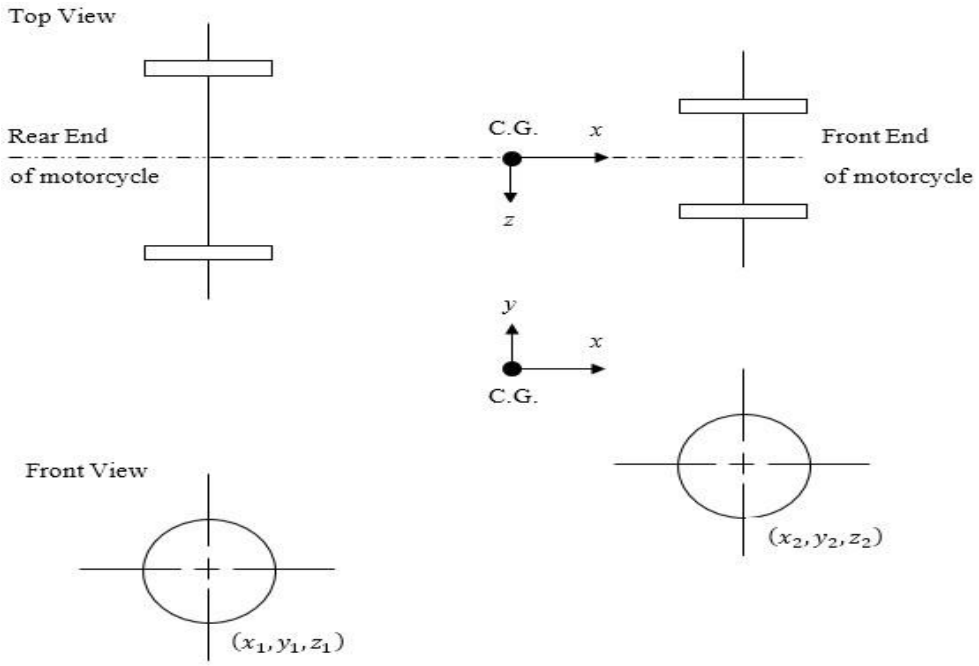

Figure 9. Schematic diagram showing the Mount System Layout

Figure 9, shows the mounting system used in this example which consists of four identical circular cross section elastomeric mounts in which, the radial and axial stiffness values fully defines the stiffness characteristics of each mount and both of these stiffness values are used as design variables. A loss factor of 0.3 and a dynamic-to-static stiffness coefficient of 1.2 have been used. In order to reduce the total number of design variables, symmetric constraints are imposed. This is done by placing two mounts on each side of the *x-y* plane resulting six position variables instead of twelve and four orientation variables instead of twelve. The radial and axial stiffness values are identical for all four mounts resulting a total of twelve design variable for the mounting system. The mass of the powertrain is 0.5 *lb-s²/in* and inertia values of the powertrain are given in Table 2.

The optimization problem is done using the SQP technique that employs an optimization routine to minimize the objective function. The design variables resulting from the optimization process are shown in Table 3. Once the operation is over, the design vector that corresponds to the optimum value of the objective function is known. The second part of the problem starts by setting the objective function described in Eq. (45) to minimize the difference between the desired stiffness values obtained from the first optimization done through the dynamic analysis and the stiffness values obtained from the geometric shape of the mount. The mount is connected to the frame via metal steel plates on both sides. These plates are bonded to the mount and the connection is at the mount attachment holes. Since the stiffness of the steel plates is higher than the mount stiffness, the constraints are moved from the plate holes directly into the mount surface as shown in Fig. 10. The boundary conditions are applied by constraining the displacement of the surface of the mount in all directions. The results of the shape optimization process are shown in Table 4. The shape optimization takes into account the range of the design variables that acts like lower and upper bounds. These bounds are shown in Eq. (52) and the starting shape of the mount and the optimized shapes are shown in Figs. 11 and 12. The resulting force plots in the x and y direction for engine speed of 4000 rpm is shown in Fig. 13 and the resulting torque plot for the engine speed of 4000 rpm is shown in Fig. 14.

$$\begin{aligned} 0.3 \le t_r \le 0.59 \\ 0.3 \le t_s \le 1.5 \\ 0.5 \le t_z \le 1.77 \\ -\pi/18 \le \theta \le -\pi/6 \end{aligned} \tag{52}$$

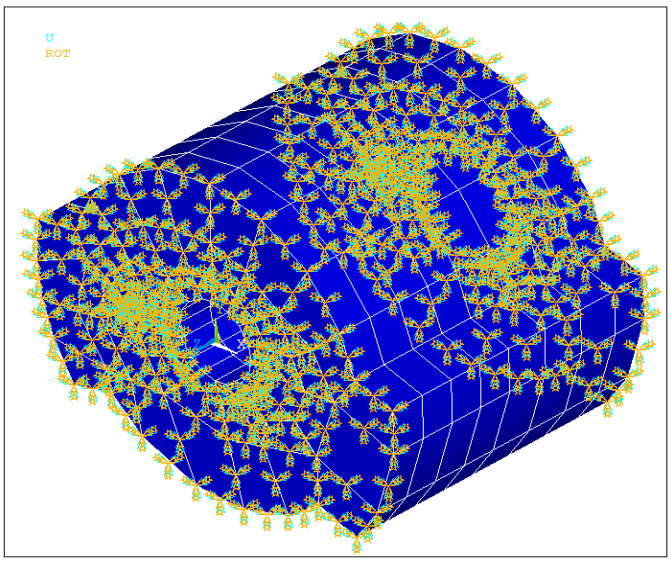

Figure10. Isometric View Showing the Boundary Conditions

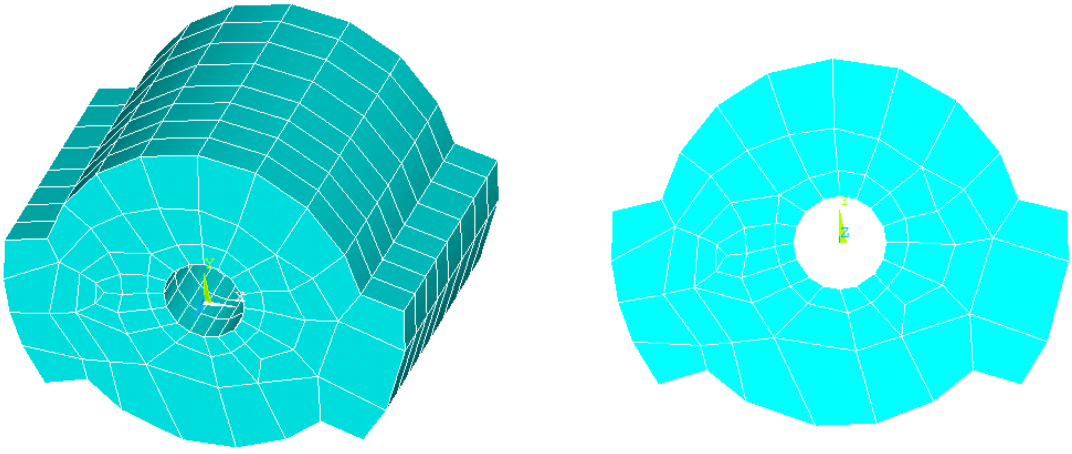

Figure 11: (a) Isometric View of the Initial Geometry, (b) Front View of the Initial Geometry

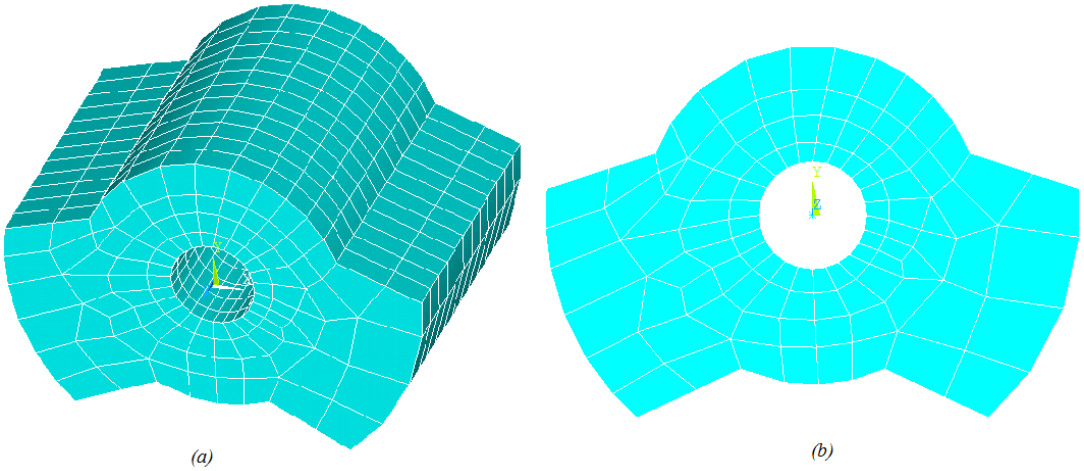

Figure 12: (a) Isometric View of the Optimized Geometry, (b) Front View of the Optimized Geometry

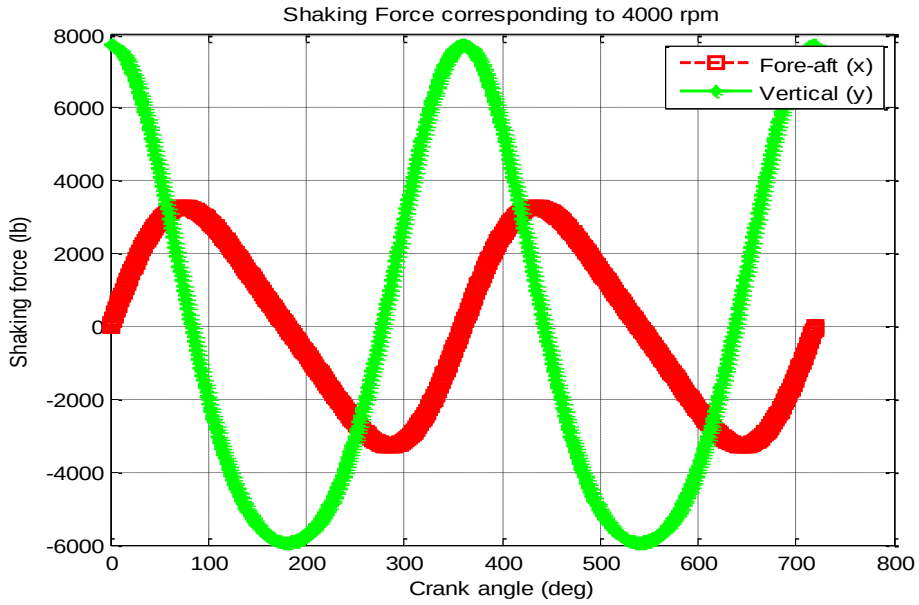

Figure 13. Shaking Force in the x and y Directions (4000 rpm)

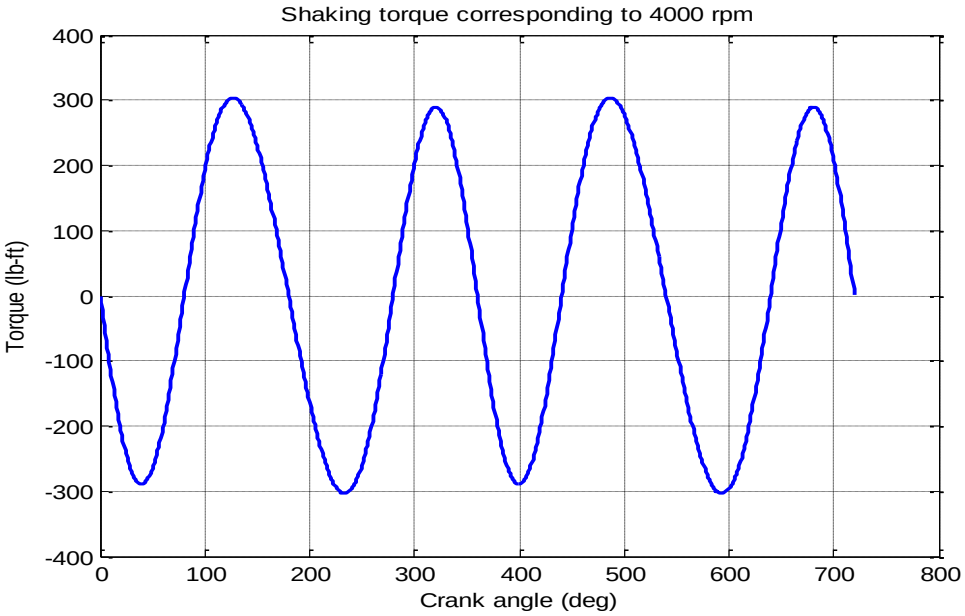

Figure 14. Shaking Torque (4000 rpm)

Table 1: Bounds for Design Variables

		Min.	Max.
Mount Stiffness (x,y)	lb/in	100	5000
Mount Stiffness (z)		500	10000
Orientation Angles	deg.	0	50

Table 2: Inertia Tensor of Powertrain Assembly.

	x	y	z
I_x	20.7	1.86	0.12
I_y	1.86	12.81	2.3
I_z	0.12	2.3	26.14

Table 3: MatLab Optimization Results.

	Load Transmitted (lb)	Mount Stiffness (lb/in)		
		x	y	z
Initial Guess	1125.32	4750	4750	2400
Optimized Design	268.60	1266.78	1266.78	4957.44

Table 4: Parameter Optimization Results

		Initial	Optimized	Target Stiffness
Design Variables	θ (rad)	6.021	5.9052	
	t_r (in)	0.591	0.4259	
	t_s (in)	0.787	0.9387	
	t_z (in)	1.378	1.4016	
Stiffness (klb/in)	kx	3.4113	1.267	1.2668
	ky	9.1838	1.271	1.2668
	kz	1.8525	4.8958	4.9574
Obj. Function	ψ	76.9188	0.0038	

CONCLUSION

The design of a shear (bush) type engine mount has been obtained using the geometrical shape optimization using the parameterization technique. The method was done through utilizing a nonlinear finite element analysis. Part of the design was done using SQP method provided by a MatLab built in function in order to find the target stiffness values. It should be noted that multiple starting guess have been used in order to determine the optimum value of the objective function in the optimization problem. This is due to the fact that the engine mount optimization problem is nonlinear and could provide local minima as a solution to the optimization problem. As it can be noticed from the results above that the optimum shape of the mount is acceptable and can be used as the final shape. It is worth mentioning that this approach is applicable for any type of engine mounts. The stiffness values that are obtained from the shape optimization are slightly different than those values obtained from the dynamic analysis; however, the shape obtained from the parametric optimization is acceptable and can be used in real design situations. A more accurate representation of the mount connection to the frame is yet to be considered in the future work.

REFERENCES

[1] ANSYS 12.0, Help Documentation, 2009, ANSYS Inc.
[2] Ashrafiuon, H., Design optimization of aircraft engine-mount systems. ASME J. Vib. Acoust., 1993, 115, 463-467.
[3] Courteille, E. and Mortier, F., 2005, “Multi-Objective Robust Design Optimization of an Engine Mounting System,” SAE, paper no. 01-2412.
[4] Ford, M. D., 1985, “An Analysis and Application of a Decoupled Engine Mount System for Idle Isolation”, SAE, paper no. 850976, pp. 133-142.
[5] Kaul, S., 2006, Modeling Techniques for Vibration Isolation in Motorcycles, PhD Thesis, University of Wisconsin, Milwaukee.
[6] Kim, J. J. and Kim, H. Y., 1997, “Shape Design of an Engine Mount by a Method of Parameter Optimization”, Computers and Structures, Vol. 65, No.5, pp. 725-731.
[7] Liu, C. Q., 2003, “A Computerized Optimization Method of Engine Mounting System”, SAE, paper no. 01-1461.
[8] MATLAB User Guide, Version 7.10, Release 2010, Math Works.
[9] Norton, R. L., 2011, Design of Machinery: An Introduction to the Synthesis and Analysis of Mechanisms and Machines, 5th edition, McGraw Hill.
[10] Rao, S. S., 2009, Engineering Optimization Theory and Practice, 4th edition, John Wiley & Sons, Chapter 7.
[11] Rivlin, R. S., 1992, “The Elasticity of Rubber”, Rubber Chem. Technol. 65, G51-G66.

[12] Snyman, J. A. and Heyns, P.S. and Vermenulen, P. J., 1995, "Vibration Isolation of a Mounted Engine Through Optimization", Mechanical and Machine Theory, Vol. 30, No.1, pp. 109-118.
[13] Spiekermann, C. E., Radcliff, C. J. and Goodman, E. D., 1985, "Optimal Design and Simulation of Vibrational Isolation Systems", Journal of Mechanisms, Transmission and Automation in Design, Vol. 107, pp. 271-276.
[14] Sui, S. J., 2003, "Powertrain Mounting design Principles to Achieve Optimum Vibration isolation with dimension Tools," Society of Automotive Engineers, paper no. 01-1476.
[15] Swanson, S. R., 1985, "Large Deformation Finite Element Calculations for Slightly Compressible Hyperelastic Materials," Computers and Structures, Vol. 21, pp. 81-88.
[16] Tao, J. S. and Liu, G. R and Lam, K. Y., 2000, "Design Optimization of Marine Engine-Mount System," Journal of Sound and Vibration, Vol. 253, No.3, pp. 477-494.